Original Article

Application of Hyperelastic-based Active Mesh Model in Cardiac Motion Recovery

Hossein Yousefi-Banaem[1,2], Saeed Kermani[1], Alireza Daneshmehr[3], Hamid Saneie[4]

[1]Department of Biomedical Engineering, Faculty of Advance Medical Technology, Isfahan University of Medical Science, [2]Medical Image and Signal Processing Research Center, Isfahan University of Medical Science, [3]Department of Cardiology, School of Medicine, Isfahan University of Medical Science, Isfahan, [4]Department of Mechanical Engineering, University of Tehran, Tehran, Iran

ABSTRACT

Considering the nonlinear hyperelastic or viscoelastic nature of soft tissues has an important effect on modeling results. In medical applications, accounting nonlinearity begets an ill posed problem, due to absence of external force. Myocardium can be considered as a hyperelastic material, and variational approaches are proposed to estimate stiffness matrix, which take into account the linear and nonlinear properties of myocardium. By displacement estimation of some points in the four-dimensional cardiac magnetic resonance imaging series, using a similarity criterion, the elementary deformations are estimated, then using the Moore–Penrose inverse matrix approach, all point deformations are obtained. Using this process, the cardiac wall motion is quantized to mechanically determine local parameters to investigate the cardiac wall functionality. This process was implemented and tested over 10 healthy and 20 patients with myocardial infarction. In all patients, the process was able to precisely determine the affected region. The proposed approach was also compared with linear one and the results demonstrated its superiority respect to the linear model.

Key words: *Heart, Humans, Infarction, Linear Models, Magnetic Resonance Imaging, Myocardium*

INTRODUCTION

Undoubtedly, biomechanical model of soft tissue is an important tool for constructing a reality-based model for less invasive simulation in medical applications. Therefore, it is necessary to consider the soft tissue as a material with special mechanical properties. The behavior of soft tissue is nonlinear in most cases. Nonlinear characteristics of soft tissues are very complicated for representing the biomechanical behavior of such materials with unique constitutive equation. However, the cost of this complexity is more accuracy in simulation results.[1] Hence, the model of soft tissue should have similar behavior to the real material. This provides estimable insights into the behavior of the soft tissue function and is helpful for heuristic preclinical research.

In the last decade, many efforts have been established to model the soft tissue motion and deformation accurately. Several models of the soft tissue including elastic, viscoelastic, hyperelastic models with different assumptions such as isotropic, transversely isotropic and orthotropic, proposed and available in the literature.[2-5] To solve soft tissue models, several computational method have been presented, that mentioned below: (1) mathematically motivated regularization methods; in these models myocardium considered as flexible thin plate with predetermined deformation manner, but myocardium is a thick wall so consideration as thin plate can't be proper for cardiac wall modeling.[6] (2) finite-element method based models.[7] (3) spatio-temporal B-spline methods; these methods are polynomial and can't represent usefully cone shape structures, like heart, but their implementation is simple and can be done with less control points.[8,9] (4) Statistical models; these models need to construct an atlas, which is a tedious task, also training with large database is necessary for these models. Training procedure has more computational cost and collecting large database is very difficult task. Advantage of these models is robustness in shape variety.[10,11] (5) Continuum biomechanics based energy minimization methods; in these methods internal

Address for correspondence:
Dr. Saeed Kermani, Department of Biomedical Engineering, Faculty of Advance Medical Technology, Isfahan University of Medical Science, Isfahan, Iran.
E-mail: kermani@med.mui.ac.ir

and external force should be known to minimize the total energy function. But in cardiac image data, the external force is unknown, and it's computation in most cases is an invasive procedure which needs pressure sensor placements in heart chamber. These models also have high computational time but in contrast are more reliable.[12-14] (6) deformable models; the main drawback of this methods is noise sensitivity. Also these methods are based on energy minimization. Some deformable methods use edge force and some methods use region intensities force. So in images with week edges and close intensities like epicardium these methods don't have reliable results, but in contrast has low computational time.[7,15-17] These methods widely have been used to regularize ill-conditioned problems in many applications such as medical image analysis. To solve the problem, material model should be assumed. In some works, the soft tissue is modeled as a linear elastic volumetric model with hexahedral and tetrahedral elements to apply continuum mechanical constraints[14,18] and in other works has modeled as nonlinear material models such as viscoelastic or hyperelastic.[3,19-22] Holzapfel *et al*. modeled left ventricular (LV) as a hyperelastic material and only tested it on experimental data with shear and biaxial deformations the advantage of this model is considering muscle fiber direction but diffusion tensor imaging of cardiac required.[23] Wu *et al*. used B-solid deformation model to estimate cardiac motion, using tagged magnetic resonance imaging (MRI) data, in which the main drawback of this model is soft tissue of myocardium considered as solid but in contrast has less complexity.[24] Hassan *et al*. applied a viscoelastic model to estimate the behavior of papillary muscle of cardiac wall That can't be generalized to the entire heart wall.[22] Linear models due to less complexity and easy implementation, widely have been used in most applications.[25,26] Nonlinear models with high complexity solved in most cases by finite element (FE) method and minimizing virtual work, which is necessary external force to be known. In medical image analysis application, external forces are unknown. Some methods introduced to solve such ill-posed problem. Jiahe Xi *et al*. solved nonlinear Guccione model by considering intra LV pressure as external force, but measuring the LV pressure is invasive task.[27] Karimi *et al*. used hyperelastic material model to estimate brain characteristic in load direction. In that study, they exposed brain and deformed it by external loading.[28] Veress *et al*. proposed hyperelastic warping technique to measure LV strains. They considered heart as a hyperelastic material and used image intensity differences as a body force, to deform the FE model in synthetic cardiac magnetic resonance imaging (CMRI).[29] Phatak *et al*. calculate LV strain by hyperelastic warping that deformation force obtained from tagged-MRI.[30] Pham *et al*. proposed an iterative procedure on an active region model that deforms and pulls towards the image edges using the FE method.[7] Among previously proposed methods, active mesh method (AMM) permits a larger number of degrees of freedom to the object.[31] AMM can merge the continuum

mechanical constrains and a great number of rules in soft tissue deformation. Object tracking in medical imaging using two-dimensional and three-dimensional (3D) AMM was introduced by Lautissier *et al*. and Kermani *et al*.[18,32] Kermani *et al*. considered LV wall as a linear elastic material and used AMM to model cardiac motion for obtaining local LV function indexes.[18,31,33]

In the previous AMMs, soft tissues considered as a linear elastic material, but as mentioned earlier its behavior is nonlinear elastic material, therefore in this study cardiac wall considered as nonlinear and hyperelastic material. Hence, in this study, a variational approach has been proposed to solve hyperelastic constitutive equations in FE framework. In this approach, both linear and nonlinear properties of material have been considered in constructing stiffness matrix. The proposed method validated by estimation cardiac motion in healthy and infarct patients. The LV myocardium considered as a homogeneous, thick-walled, incompressible, and transversely isotropic nonlinearly elastic material, which adopted in the current study.

This paper is organized as follows: Representing nonlinear AMM (NLAMM) with hyperelastic constitutive relations and data fitting. Section 3 shows the results of AMM method which described in Section 2, and applied for cardiac motion recovery, Sections 4 offer discussion on obtained results from NLAMM and Sections 5 represent the conclusion.

METHODS

To solve the NLAMM, an energy minimization approach has been applied. In the following first image acquisition segmentation, 3D template construction and point tracking will be defined briefly then total energy of deformation was defined and constitutive relation of hyperelastic material for obtaining stiffness has been demonstrated and finally by minimizing the total energy model has been fitted to the displacement. In the fitting procedure, two terms have been used, one is regularization term which was obtained from strain energy function another is fitting term that was obtained from estimated error between displacement of points which was calculated by tracking algorithm and estimated by model. For evaluation, proposed approaches have been used for cardiac motion analysis. The graphical block diagram of NLAMM based cardiac motion recovery is sketched in Figure 1.

Data Acquisition

Real patient geometric data with myocardial infarct was selected from three cine MRI databases. Eleven Gradient-Echo images were performed on a 1.5 T scanner (Symphony Siemens, Germany) located at Isfahan MRI Center, Isfahan, Iran.[18] Ten of them obtained from Sunnybrook Health Sciences Centre, Toronto, Canada with resolution 256 × 256 × 10 × 20[34]
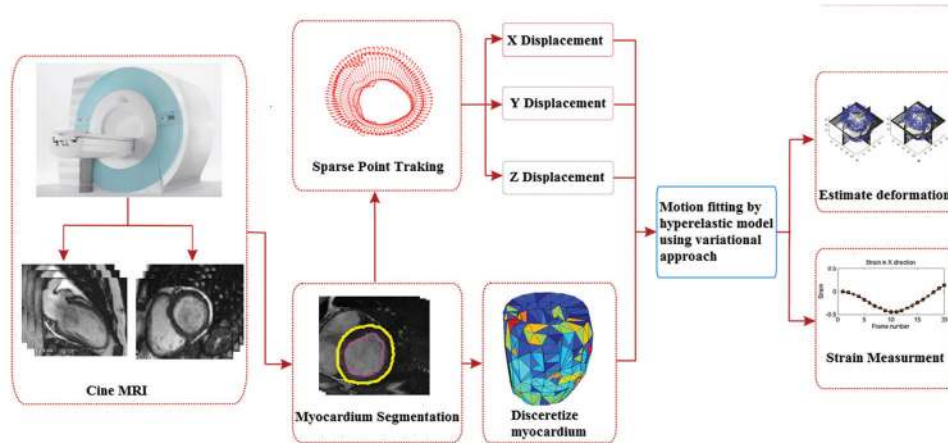
Figure 1: Graphical block diagram of nonlinear active mesh method based cardiac motion recovery

and 10 of them obtained from cardiac atlas project.[35] The implemented MATLAB program runs in a computer with dual-core 2.53 GHz CPU and 16G of RAM.

Segmentation

Epi/endocardial of all slices in all frames are segmented exactly based on the algorithm introduced by Heiberg *et al.*[36] This method is developed on the concept of deformable models but extended with an enhanced and fast edge detection scheme that includes temporal information, and anatomical a priori knowledge. In this method, LV considered as an open "cone," which sliced along its long axis with an equal 80 points for each slice. But results of this algorithm aren't accurate among all slices and frames, so all segmentation was refined by an expert until contours coincide to the epi/endocard.

Template Constructing

A volumetric 3D template of LV was made using quick hall algorithm. A fast and quite simple algorithm to create a convex hull of a huge number of 3D points is the quick-hull algorithm. Here's a short overview of its implementation. For mesh-representation, half edge data structure was used. It allows fast queries on any kind of neighboring mesh-elements and also fast mesh-modifications. This algorithm builds meshes in two phases as described here:[37]
1. Initial phase: In this phase initial tetrahedron is created, and then points assigned to the faces, finally faces without points are ignored
2. Iteration phase: This step constructed as below: Get most distant point of the face's point-set, then find all faces that can be seen from that point, after that extract horizon edges of light-faces and extrude to point, and then assign all points off all light-faces to the new created faces finally push new created faces on the stack, and start iteration phase again. Faces without points are ignored.

To make the template, the points on the external and internal surface of the template are determined by:

$$X_{Temp} = \begin{cases} X + sgn(XC - X), X \in Endocardial\ surface \\ X - sgn(XC - X), X \in Epicardial\ surface \end{cases}$$

Where *XC* is the endo/epicardial centroid of its slice, *X* = (*x*, *y*, *z*) is the coordinate point which belongs to endo/epicardial layer and X_{Temp} is the respected template point.

Spares Field Tracking

To obtain the sparse field of displacement, the point on the epi/endocardial surfaces were used. To track the point displacement and determination of the initial spares motion field, an efficient block matching algorithm is used based on normalized mutual information (NMI). This approach implemented on two sequential frames of a 3D sequence image. To do this first, 3D mask with center of the selected points in current frame image was selected, and then NMI between 3 × 3 × 3 window with the center of the given point and 3 × 3 × 3 window of the correspondent candidate points was computed, finally the point which has the maximum NMI, as the correspondent point was selected.

Nonlinear Active Mesh Method

Hyperelastic constitutive
For obtaining the deformations of the cardiac wall, the boundary surface of the cardiac wall is extracted from the reference frame. Then, obtained face is approximated by a polyhedron. The vertices of the polyhedron are fed to a 3D Delaunay triangulation algorithm, while outputs are a list of vertices and a list of tetrahedral elements. Let *T* = {*V*, *F*} be a tetrahedral defined over the object region, where *F* is a set of tetrahedral elements and *V* is a set of tetrahedral vertices.

To fit the model to the experimental data, an energy function was defined, and then this function was minimized according to the displacements to obtain all point deformations. The global energy function defined as sum of internal and data energy function as:[18]

$$E = E_{int} + E_{Data} \tag{1}$$

The 3D object is then modeled as an incompressible 3D hyperelastic material which deforms with the virtual forces. From FE theory, the strain energy in continuous form is given by:

$$E_{int} = \int_{\Omega_0} \sigma \varepsilon d\Omega \tag{2}$$

In hyper-elastic material relation between strain and stress is not linear and stress obtained by differentiates the strain energy function according to the strain. As we define W (ε) as below:

$$W(\varepsilon) = W(J_1, J_2, J_3) \tag{3}$$

Where J_1, J_2, J_3 are the invariants of strain. Stress obtained by differentiates the strain energy function according to the strain as:

$$\sigma = \frac{\partial W}{\partial \varepsilon} \tag{4}$$

By substituting Eq. 4 in the Eq. 2 we obtain:

$$E_{int} = \int_{\Omega_0} \frac{\partial W}{\partial \varepsilon} \varepsilon d\Omega \tag{5}$$

The nonlinear variational equation cannot be solved easily due to the nonlinearity involved in the displacement–strain relation. Tangent line at the current solution, it is often called a tangent stiffness, and the process is called linearization. Linearization of the energy form in Eq. 5 can be written as:[38]

$$L(E_{int}) = \int_{\Omega_0} (\Delta S : E + S : \Delta E) d\Omega \tag{6}$$

Where ΔS is the stress increment and ΔE is the increment of strain variation and: Represent the contraction operator. For the hyper-elastic material the increment of stress can be written as:

$$\Delta S = \frac{\partial S}{\partial E} : \Delta E = D : \Delta E \tag{7}$$

Where D is the fourth-order constitutive tensor and obtained by:

$$D = \frac{\partial S}{\partial E} = \frac{\partial W(E)}{\partial E \partial E} \tag{8}$$

Thus, the linearization of the energy form in Eq. 5 can be explicitly derived with respect to displacement and its variation as:

$$L(E_{int}) = \int_{\Omega_0} (E : D : \Delta E + S : \Delta E) d\Omega \tag{9}$$

The variation of Lagrangian strain E in Eq. 9 can be written in vector notation as:

$$E = B_N d \tag{10}$$

Where $\{d_1, d_2, d_3, \ldots, d_n\}$ is the variation of nodal displacements and B_N is the nonlinear displacement–strain matrix defined as:[38]

$$B_N = \begin{pmatrix} N[i,j]F[k,l] \\ N[i,j]F[k,l] + N[l,j]F[i,k] \end{pmatrix}_{i,k,l=1\ldots3,\, j=1\ldots4} \tag{11}$$

Then, the first term in the structural energy form can be written as:

$$\int_{\Omega_0} E : D : \Delta E d\Omega = d^T \left(\int_{\Omega_0} [B_N]^T [D][B_N] d\Omega \right) d \tag{12}$$

Note that the nonlinear displacement–strain matrix B_N is clearly different from B in linear systems. Since B_N is the nonlinear displacement–strain matrix, it can consider the nonlinear properties of myocardium. Deformation field estimation can be improved using it in comparison of B linear. The second term, the initial stiffness, of the linearized energy form can be written as:

$$\int_{\Omega_0} S : \Delta E d\Omega = d^T \left(\int_{\Omega_0} [B_G]^T [\Sigma][B_G] d\Omega \right) d \tag{13}$$

Where B_G and $\sum$ obtained as:[38]

$$B_G = \begin{bmatrix} N_{i,j} & 0 \\ 0 & N_{i,j} \end{bmatrix} \tag{14}$$

$$\Sigma = S \otimes \delta_{ij} \tag{15}$$

Where $\otimes$ represents the Kronecker tensor product and S is stress matrix.

Using Eq. 12 and Eq. 13, the tangent stiffness matrix can be calculated as:

$$K_T = \int_{\Omega_0} \left([B_N]^T [D][B_N] + [B_G]^T [\Sigma][B_G] \right) d\Omega \tag{16}$$

Discretization of continuous material has done using FE method which the object was divided into smaller elements finally the internal energy can be computed as:

$$E_{Strain} = \frac{1}{2} d^T K_T d \tag{17}$$

$$d = [..dx_i.. | ..dy_i.. | ..dz_i..], \, i = 1, 2, \ldots N$$

Data energy was calculated as mean square error of estimated and correspondence point as following Eq. 18:

$$E_{Data} = \sum_{i=1}^{N} \lambda_i^2 || d_i - \delta_i ||^2 \tag{18}$$

Where I = 1… N and $\delta_i = (\delta x_i, \delta y_i, \delta z_i)$.

Data Fitting

By estimation of the displacement of some points of the image in next frame using a similarity criterion, the elementary deformations U may be estimated using the least squares approach. $\delta_i = (\delta x_i, \delta y_i, \delta z_i)$ is the estimation of displacement of point $(\hat{x}_i, \hat{y}_i, \hat{z}_i)$.

$$\min_d \left\{ \sum_{i=1}^{M} \| d_i - \delta_i \|^2 + d^T K_T d \right\} \tag{19}$$

Where d_i is the displacement vector, which is obtained from the model fitting procedure and δ_i is the displacement vector, which is obtained from the point correspondence procedure. For a point P in the tetrahedron $\Delta P_k P_l P_n$, the deformation function $d(x, y, z)$ is calculated by linear interpolation from neighboring elementary deformation vectors using:[31]

$V(\cdot)$, is the volume calculation function.

Using Eq. 13, the above minimization is seen to be equivalent to the minimization:

$$\min_d \left\{ \| Ad - B \|^2 + d^T K_T d \right\} \tag{20}$$

$$B = [\ldots \delta x_i \ldots | \ldots \delta y_i \ldots | \ldots \delta z_i \ldots]^T, \delta_i = (\delta x_i, \delta y_i, \delta z_i)$$

$$A = \begin{pmatrix} Q & 0 & 0 \\ 0 & Q & 0 \\ 0 & 0 & Q \end{pmatrix}_{3m \times 3n}$$

$$Q_{ij} = \begin{cases} g_j(\hat{x}_i, \hat{y}_i, \hat{z}_i), j = \{r, s, t, u\} \text{ if} \\ \qquad (\hat{x}_i, \hat{y}_i, \hat{z}_i) \in \Delta P_r P_s P_t P_u \\ 0 \qquad , \text{ otherwise} \end{cases} \tag{21}$$

The solution to Eq. 19 is Eq. 22, which gives the displacement of all vertices of the mesh. Then, the displacement of all points of LV muscle will be obtained by interpolation. Eq. 20 is a regularization term and solved by Moore–Penrose inverse matrix.

$$\hat{d} = (A^T A + K_T)^{-1} A^T B \tag{22}$$

Application to Cardiac Motion Analysis

For evaluating proposed method cardiac wall motion estimated. In this procedure cardiac wall has adopted as Mooney–Rivlin hyperelastic model to consider; nonlinearly properties of cardiac wall. Also, LV wall assumed to be homogeneous and incompressible. The strain energy function of LV wall defined as below:

$$W(J_1, J_2, J_3) = A_{10}(J_1 - 3) + A_{01}(J_2 - 3) + \frac{K}{2}(J_3 - 3)^2 \tag{23}$$

Where A_{10}, A_{01} and K are material constants related to the distortional and volumetric response respectively. Invariants J_1, J_2, J_3 obtained by:

$$J_1 = I_1 (I_3)^{-1/3}$$
$$J_2 = I_2 (I_3)^{-2/3} \tag{24}$$
$$J_3 = (I_3)^{1/2}$$

Where I_1, I_2 and I_3 are invariant of left green-cushy deformation gradient tensor and obtained from:

$$I_1 = \text{trace}(B) = B_{kk}$$
$$I_2 = \frac{1}{2}(I_1^2 - B.B) = \frac{1}{2}(I_1^2 - B_{ik} B_{ki}) \tag{25}$$
$$I_3 = \det B = J^2$$

Where B is the green-cushy deformation gradient tensor that measured by:

$$B = FF^T \tag{26}$$

And F is deformation gradient and calculated by:

$$F_{ij} = \delta_{ij} + \frac{\partial u_i}{\partial x_j} \tag{27}$$

Where δ_{ij} is Kronecker delta and u_i is deformation.

RESULTS

Considering nonlinearity of myocardium in modeling procedure, can improve the cardiac wall assessment. Therefore, this study established to develop analytical method to solve nonlinear material model by using variational approach and FE method. Validation of method has been done by estimating LV wall motion in healthy and infarct patients.

To assess the myocardium, 3D template construction of LV is required. For this reason LV wall was segmented in all slices over all frames from end-diastole to end-systole as shown in Figure 2.

Moreover, the obtained boundaries in end-diastole fed to convex-hall algorithm to build surface template of LV wall. Finally, vertex of the triangulated surface served to tetgen software to tetrahedralize LV wall as shown in Figure 3.

After LV meshing all displacement of cardiac wall estimated using the proposed method which was described in Section 2, LV wall motion over cardiac cycle estimated and deformed mesh of LV wall constructed. Deformation of LV from end-diastole to end-systole has been showed in Figure 4.

To represent LV wall tracking by the model, the deformed mesh by model was visualized with three plan of cardiac
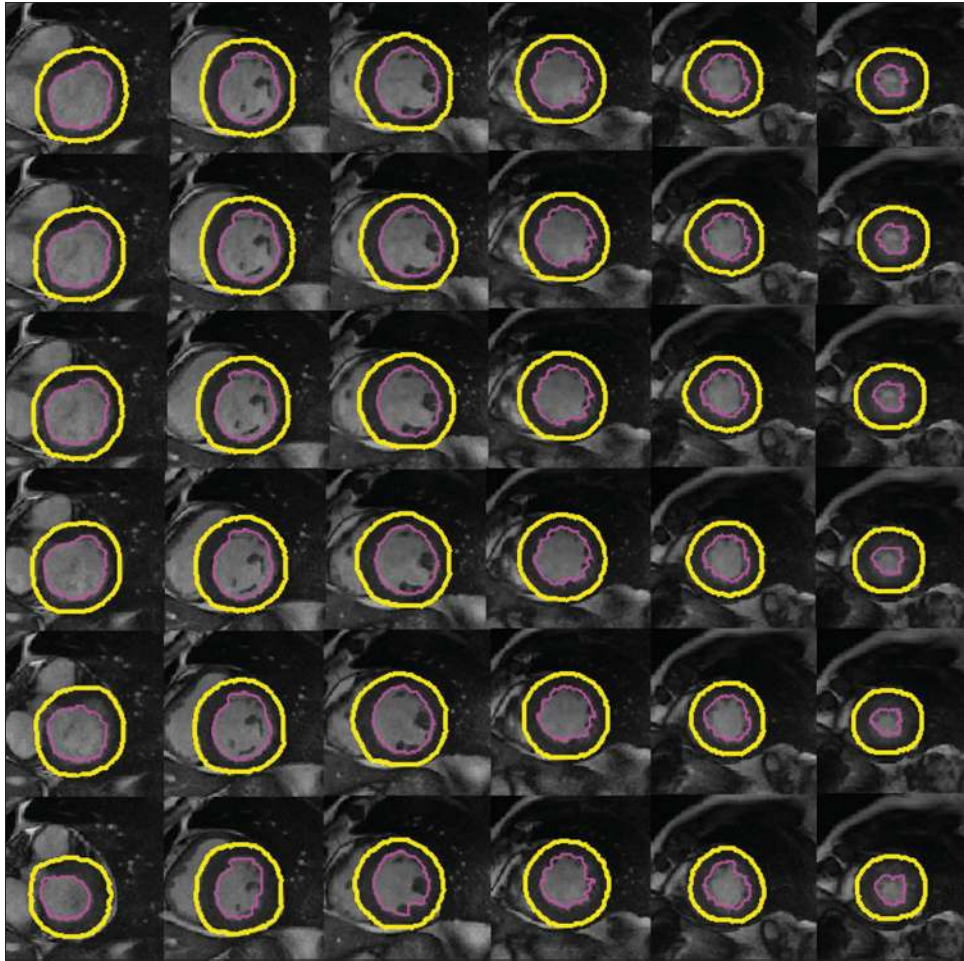
Figure 2: Segmentation cine CMRI data from basal (left) to apex (right) over all frame from end diastole (up) to end systole (bottom). The mean resolution of data is 256 × 256 × 10 × 20
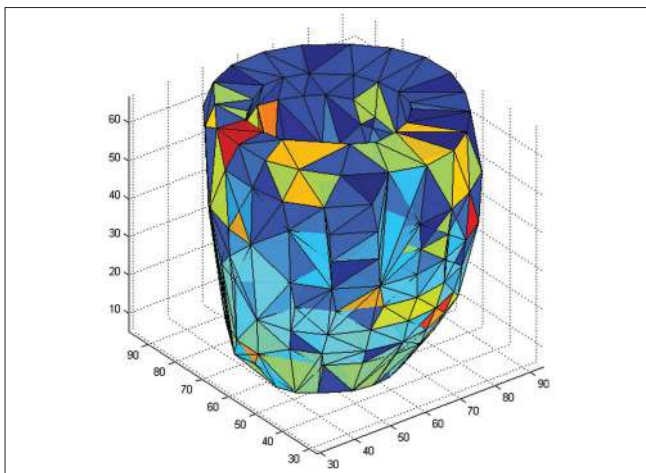
Figure 3: Cardiac wall template meshing, cardiac wall template has meshed by open source Tetgen software and visualized in MATLAB. This template consists of 1275 tetrahedral elements and 430 vertexes. Each element presented in different color

LV wall in X, Y and Z directions. As showed in Figure 5, the deformed meshes were well matched to the LV wall.

Also, a movie of this deformation was created to show the deformation of the model frame by frame.

Strain in healthy regions is different than infarct regions. Strain was computed over all frames for each tetrahedral element and the results are depicted in Figure 6; all are consistent with the clinical evidence. Representation of object deformation in model space enables strain-displacement analysis in local object coordinates and patient-specific analysis of LV wall motion.

DISCUSSION

In current study, we proposed a method to fit a model to the data by considering material as a hyperelastic. In the proposed method, solution obtained by minimizing total energy function that constructed of two terms. One is regularization term which derived from strain energy function and second term is fitting term that defines as absolute mean square error between real data point and estimated points by the model. For constructing the stiffness
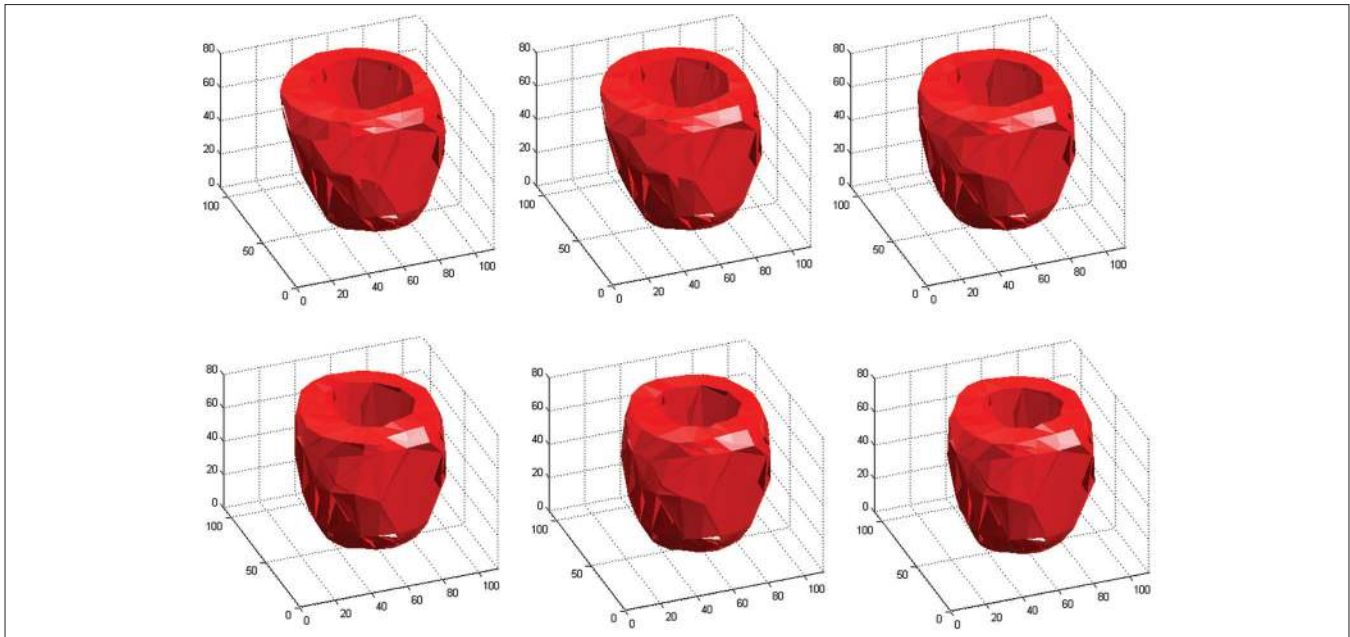
Figure 4: Deformation of template mesh from end diastole to end systole. A is the reference frame at end diastole and F is the deformed mesh in end systole, B, C, D, E are the frames between reference frame and deformed frame. This procedure shows the tracking the left ventricular wall motion by the model
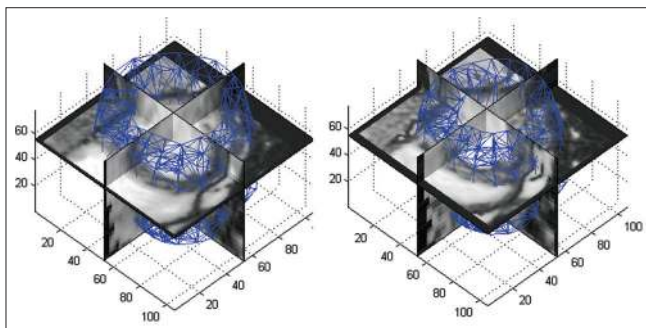

Figure 5: Deformation mesh from end diastole to end systole along with cardiac magnetic resonance imaging. A is the reference frame at end diastole and B is the deformed mesh in end systole that presented in 3 plane of cardiac magnetic resonance imaging image series

matrix, nonlinear and linear strain-displacement matrix as defined in Eq. 11 and Eq. 14 has been used. Therefore, in the proposed approach, both linear and nonlinear properties of the material have been considered by calculating linear and nonlinear strain-displacement relation matrix. Considering both linear and nonlinear properties of soft tissue enable us to model soft tissue behavior more reliable than linear ones. Validation of proposed methods is a tedious task and require implanted markers in deforming body as cardiac wall, or special experiments, which may not be feasible in practice.

To better understand the model behavior, proposed method was evaluated by estimating LV wall motion. Some points were tracked from end diastole to end systole by efficient block matching algorithm that called sparse motion field. Then by fitting a model to the sparse field, the motion of all points (dense motion field) of cardiac wall estimated.

For simplicity LV wall considered as incompressible, transversely isotropic and homogenous Mooney Rivilin hyperelastic material. As shown in Figures 4 and 5, proposed approach could track cardiac wall motion from end diastole to end systole. Deformation of meshes warped to the cardiac wall during the heart period and results of the model well matched to the data. For evaluation of method in detecting healthy and infarct, area of heart strain was calculated and sketched versus displacement as shown in Figure 6. Obtained results showed a regular pattern and nonlinear relation between strain and displacement in healthy case and irregular pattern and strain-displacement relation in infarct cases. Absolute value of strain increased by displacements in healthy cases as expected, but in the infarct patients due to wall defect strain have less amplitude and more irregularity in comparison of healthy one. In compare with other nonlinear methods which were used by Xi *et al*. our method has less complexity and cost. They have used Cine and tagged MRI simultaneously to estimate the dense motion field. Therefore, patient MRIs were taken with two separate protocols: Tagged and Cine. This method has two disadvantages, first: Agitation and patient discontent, second: Being expensive and time-consuming. However, our proposed method estimate the dense motion field only from Cine MRI which takes two times less than nonlinear method method proposed by Xi *et al*., and the cost is also reduced by half. Also, they have used fiber based model without having fiber direction which were obtained from diffusion weighted imaging.[19] The proposed approach was compared with linear AMM method that has been used in Kermani *et al*. work.[18] The complexity of our method due to computation of B_N (nonlinear) and B_G (linear) is at least two times more than linear method used in Kermani *et al*.
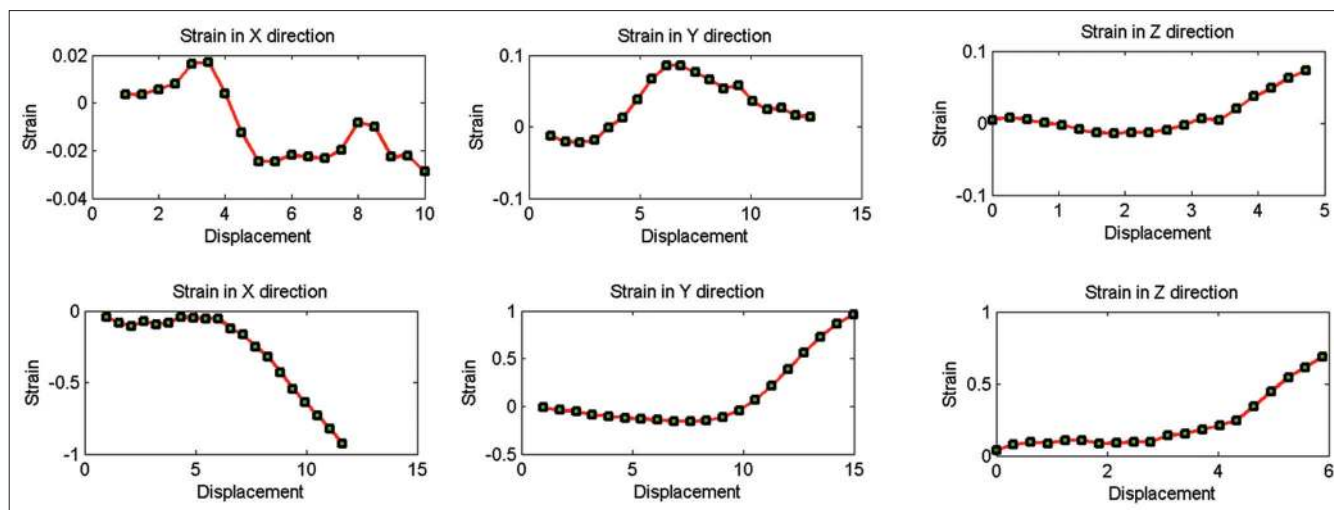
Figure 6: Strain-displacement relations in healthy and patient data. Upper row belong to the infarct patient as expected due to left ventricular wall abnormality in this patients, strain has less amplitude and is irregular. Lower row related to the healthy one, as expected it is regular, also has higher amplitude in comparison to the infarct patient and absolute value of strain increased as displacement increased

Table 1: Error table of proposed method

	RMSE (f)		Absolute error (mm)	
	Mean	SD	Mean	SD
Proposed method	9.072	4.637	0.146	0.119
Linear	13.252	5.480	0.161	0.128

RMSE (f) is mean square errors in the fth frame. Absolute error is the error of real data point and corresponds estimated point. SD: Standard deviation, RMSE: Root mean square error

However in contrast the proposed method has minimal error. For comparison of two methods, RMSE error and absolute error between real data points and estimated points were calculated as shown in Table 1.

For validation of this method, results were compared with angiography, cardiac perfusion scan and electrocardiogram data of patients. All findings demonstrated that our proposed method was able to assess the myocardium with consistent clinical evidence.

CONCLUSION

Hyperelastic cardiac wall functionality was evaluated by a variational approach which was proposed to calculate stiffness matrix to minimize the total energy. Then, by estimating the dense motion field of cardiac wall points using NLAMM, local parameters were estimated. As demonstrated earlier this approach considers both linear and nonlinear properties of soft tissue so as expected it had better results than linear model. The results from NLAMM on healthy and patient data set were consistent with the clinical evidence of that patient. Also, obtained strain well matched with data information. Therefore, variational approach with combination of AMM is recommended to solve ill-posed problem in cardiac image analysis.

Conflicts of Interest

There are no conflicts of interest.

REFERENCES

1. Yingchoncharoen T, Agarwal S, Popovic ZB, Marwick TH. Normal ranges of left ventricular strain: A meta-analysis. J Am Soc Echocardiogr 2013;26:185-91.
2. Petitjean C, Dacher JN. A review of segmentation methods in short axis cardiac MR images. Med Image Anal 2011;15:169-84.
3. Vese LA, Chan TF. A multiphase level set framework for image segmentation using the Mumford and Shah model. Int J Comput Vis 2002;50:271-93.
4. Yousefi-Banaem H, Kermani S, Sarrafzadeh O, Khodadad D. An improved spatial FCM algorithm for cardiac image segmentation. in Processing. 13th Iranian Conference on Fuzzy Systems; 2013.
5. Oberhuber T, Kučera S, Loucký J, Súkupová L, Tintěra J. Segmenting tagged cardiac MRI data using a local variance filter. Acta Polytechnica 2014;54:214-20.
6. Shi P, Sinusas AJ, Constable RT, Ritman E, Duncan JS. Point-tracked quantitative analysis of left ventricular surface motion from 3-D image sequences. IEEE Trans Med Imaging 2000;19:36-50.
7. Pham Q, Vincent F, Clarysse P, Croisille P, Magnin I. A FEM-Based Deformable Model for the 3D Segmentation and Tracking of the Heart in Cardiac MRI. Proceedings of the 2nd International Symposium on Image and Signal Processing and Analysis, Pula:IEEE; 2001.
8. Tustison NJ, Dávila-Román VG, Amini AA. Myocardial kinematics from tagged MRI based on a 4-D B-spline model. IEEE Trans Biomed Eng 2003;50:1038-40.
9. Huang J, Abendschein D, Dávila-Román VG, Amini AA. Spatio-temporal tracking of myocardial deformations with a 4-D B-spline model from tagged MRI. IEEE Trans Med Imaging 1999;18:957-72.
10. Frangi AF, Rueckert D, Schnabel J, Niessen WJ. Automatic

construction of multiple-object three-dimensional statistical shape models: Application to cardiac modeling. IEEE Trans Med Imaging 2002;21:1151-66.

11. Lötjönen J, Kivistö S, Koikkalainen J, Smutek D, Lauerma K. Statistical shape model of atria, ventricles and epicardium from short- and long-axis MR images. Med Image Anal 2004;8:371-86.

12. Bistoquet A, Oshinski J, Skrinjar O. Left ventricular deformation recovery from cine MRI using an incompressible model. IEEE Trans Med Imaging 2007;26:1136-53.

13. Nordsletten DA, Niederer SA, Nash MP, Hunter PJ, Smith NP. Coupling multi-physics models to cardiac mechanics. Prog Biophys Mol Biol 2011;104:77-88.

14. Papademetris X, Sinusas AJ, Dione DP, Constable RT, Duncan JS. Estimation of 3-D left ventricular deformation from medical images using biomechanical models. IEEE Trans Med Imaging 2002;21:786-800.

15. Montagnat J, Delingette H. 4D deformable models with temporal constraints: Application to 4D cardiac image segmentation. Med Image Anal 2005;9:87-100.

16. Park J, Metaxas D, Axel L. Analysis of left ventricular wall motion based on volumetric deformable models and MRI-SPAMM. Med Image Anal 1996;1:53-71.

17. Zhu Y, Papademetris X, Sinusas AJ, Duncan JS. A coupled deformable model for tracking myocardial borders from real-time echocardiography using an incompressibility constraint. Med Image Anal 2010;14:429-48.

18. Kermani S, Moradi MH, Abrishami-Moghaddam H, Saneei H, Marashi MJ, Shahbazi-Gahrouei D. Quantitative analysis of left ventricular performance from sequences of cardiac magnetic resonance imaging using active mesh model. Comput Med Imaging Graph 2009;33:222-34.

19. Anami BS, Unki PH. A Combined Fuzzy and Level Sets' Based Approach for Brain MRI Image Segmentation. In: Computer Vision, Pattern Recognition, Image Processing and Graphics (NCVPRIPG), 2013 Fourth National Conference on. Jodhpur: IEEE; 2013.

20. Katz MJ, Ness SM. Coronary Artery Disease (CAD). California, USA: Wild Iris Medical Education, Inc.; 2015.

21. Wang H, Amini AA. Cardiac motion and deformation recovery from MRI: A review. IEEE Trans Med Imaging 2012;31:487-503.

22. Hassan MA, Hamdi M, Noma A. The nonlinear elastic and viscoelastic passive properties of left ventricular papillary muscle of a guinea pig heart. J Mech Behav Biomed Mater 2012;5:99-109.

23. Holzapfel GA, Ogden RW. Constitutive modelling of passive myocardium: A structurally based framework for material characterization. Philosophical Transactions of the Royal Society of London A: Mathematical, Physical and Engineering Sciences. 2009;367:3445-75.

24. Wu H, Heng PA, Wong TT. Cardiac motion recovery using an incompressible B-solid model. Medical engineering & physics. 2013;35:958-68.

25. Banaem HY, Ahmadian A, Saberi H, Daneshmehr A, Khodadad D, Brain tumor modeling: Glioma growth and interaction with chemotherapy. 2011 International Conference on Graphic and Image Processing. Int Soc Optics Photonics 2011. doi:10.1117/12.913432.

26. Yousefi H, Ahmadian A, Khodadad D, Saberi H, Daneshmehr A. An optimised linear mechanical model for estimating brain shift caused by meningioma tumours. Int J Bio Sci Eng 2013;1:1-9.

27. Xi J, Lamata P, Niederer S, Land S, Shi W, Zhuang X, *et al*. The estimation of patient-specific cardiac diastolic functions from clinical measurements. Med Img Anal 2013;17:133-46.

28. Karimi A, Navidbakhsh M, Yousefi H, Haghi AM, Sadati SA. Experimental and numerical study on the mechanical behavior of rat brain tissue. Perfusion 2014;29:307-14.

29. Veress AI, Gullberg GT, Weiss JA. Erratum: Measurement of Strain in the Left Ventricle during Diastole with cine-MRI and Deformable Image Registration. J Biomech Eng 2005:127:1195-207.

30. Kermani S, Moradi M, Abrishami-Moghaddam H, Saneei H, Marashi-Shoshtari M. 3D Point Wise Tracking of the Left Ventricle over Cardiac Image Sequences Using Active Mesh and Physical Models. J Appl Sci 2008;8:4500-11.

31. Dinan FJ, Mosayebi P, Moghadam HA, Giti M, Kermani S. A fully 3D system for cardiac wall deformation analysis in MRI data. Functional Imaging and Modeling of the Heart. Springer Berlin Heidelberg; 2007. p. 12-21.

32. Lautissier J, Legrand L, Lalande A, Walker P, Brunotte F, editors. Object tracking in medical imaging using a 2D active mesh system. Proceedings of the 25th Annual International Conference of the Engineering in Medicine and Biology Society. Cancun, Mexico: IEEE; 2003.

33. Khajehpour H, Kermani S, Hashemi M, Karami M. Heart Motion Estimation Using a Deformable Model and Multislice Computerized Tomography Images. J Isfahan Med Sch 2013 31:521-31.

34. Alfakih K, Plein S, Thiele H, Jones T, Ridgway JP, Sivananthan MU. Normal human left and right ventricular dimensions for MRI as assessed by turbo gradient echo and steady-state free precession imaging sequences. J Magn Reson Imaging 2003;17:323-9.

35. Fonseca CG, Backhaus M, Bluemke DA, Britten RD, Chung JD, Cowan BR, *et al*. The cardiac atlas project – An imaging database for computational modeling and statistical atlases of the heart. Bioinformatics 2011;27:2288-95.

36. Heiberg E, Wigström L, Carlsson M, Bolger A, Karlsson M. Time resolved three-dimensional automated segmentation of the left ventricle. In: Computers in Cardiology. Lyon: IEEE; 2005.

37. Barber CB, Dobkin DP, Huhdanpaa H. The quickhull algorithm for convex hulls. ACM Trans Math Softw 1996;22:469-83.

38. Sugeng L, Mor-Avi V, Weinert L, Niel J, Ebner C, Steringer-Mascherbauer R, *et al*. Quantitative assessment of left ventricular size and function side-by-side comparison of real-time three-dimensional echocardiography and computed tomography with magnetic resonance reference. Circulation 2006;114:654-61.